

Introduction to MT-DIW2 Special Issue

Alan G. JONES¹ and Adam SCHULTZ²

¹*Geological Survey of Canada, 1 Observatory Crescent, Ottawa, Ontario, Canada, K1A 0Y3*

²*Institute of Theoretical Geophysics, Department of Earth Sciences, University of Cambridge, Downing Street, Cambridge, England, CB2 3EQ*

1. Introduction

The second Magnetotelluric Data Interpretation Workshop (MT-DIW2) was held at the University of Cambridge, England, on August 5th and 6th, 1994. MT-DIW2 was timed to be just prior to the 12th Workshop on Electromagnetic Induction in the Earth, held in Brest, France, from August 8th–13th.

The MT-DIW2 follows on from the successful MT-DIW1 (Jones, 1993a) held in Wellington, New Zealand, in 1992. A total of thirty-five scientists from ten countries attended the workshop, and gave twenty-six contributions. The following twelve papers are a subset of those twenty-six. Other contributions have been published independently of this special issue.

Following the practise established at the MT-DIW1, prior to the workshop datasets were chosen for analysis by all participants. Indeed, the entry fee to the workshop was a commitment to undertake some examination of one of more of the datasets. A total of four datasets were chosen. Two of these had been those examined at the MT-DIW1, namely the COPROD2 dataset (Jones, 1993b) (3 contributions) and the BC87 dataset (Jones, 1993c) (5 contributions). Aspects of these were left unanswered after the MT-DIW1, and accordingly they were examined again. Two new datasets were taken, both from industry, and are described briefly below. One of these was from a small survey along a single profile in Papua New Guinea (PNG) (14 contributions) provided by Chevron (Australia) Ltd. There was a well-defined geological question that needed to be addressed. The other was from an EMAP survey in Oklahoma (OKEMAP) (4 contributions) provided by Exxon Ltd. Again, the question asked was relatively simple.

During the two days, intensive discussion and examination of all four datasets was augmented by access to graphics workstations and to the Geotools MT data analysis and presentation software. This engendered a workshop-like environment and an atmosphere of free exchange between all participants.

Below we describe briefly the two new datasets, and give an overview of the following twelve papers, two on COPROD2, two on BC87, two on OKEMAP, and six on PNG.

2. OKEMAP Dataset

The OKEMAP dataset comprise a 30-km-long NE-SW EMAP line, with four MT sites in the vicinity of the line, near Madill, south-central Oklahoma (Fig. 1), acquired by Zephyr Geophysical Services for Exxon. The EMAP dipoles were mostly 1000 ft (~300 m) in length. The geology in the middle of the line consists of a thrust section with layered stratigraphy at either ends. The local geology is described in Hart (1974).

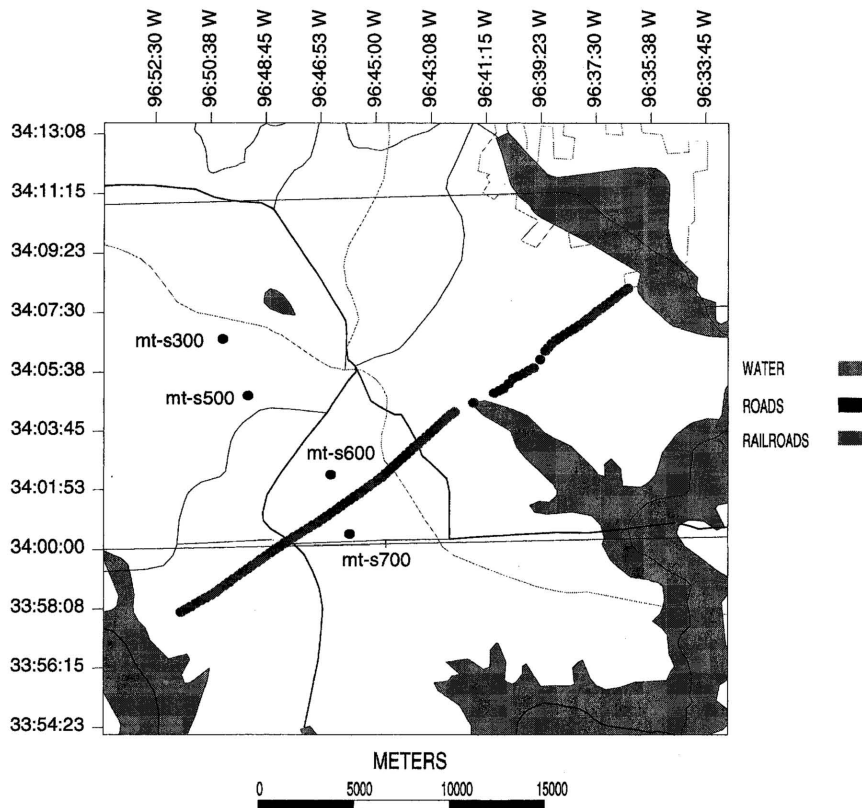


Fig. 1. Location map of the OKEMAP dataset sites. The NE-SW line of sites is the EMAP line, with 300 m dipoles. In-line electric fields only were recorded on this line. The four full 5-component MT sites also shown.

3. PNG Dataset

The PNG dataset comprise MT data in the frequency range 0.00549 Hz (1820 s)–384 Hz acquired at ten sites along a 5.6-km-long NNE-SSW profile in the Kube Kabe ranges of the highlands of Papua New Guinea (Fig. 2). The acquisition report provided by the contractor, Zephyr Geophysical Services, is appended below. The data were provided by Bill Robinson of Chevron (Australia) through an approach made on behalf of the EM induction community by Charlie Swift (Chevron, U.S.A.).

The Darai limestone outcrops as a series of multiply thrust-faulted anticlinal structures, and provides traps for the oil within the underlying Toro sandstone. The basic question asked of the MT data is to resolve whether there is a double thickness of Darai limestone caused by thick-skinned thrusting along the Soro Thrust (model B, Fig. 3), or whether there is only a single layer of Darai beneath the profile as a result of thin-skinned thrusting along the Soro Thrust (model A, Fig. 3). The geometry of the anticlinal trapping structures in the Toro reservoir is obviously very dependent on the style of thrusting.

A well drilled close to the line (Wara-1, Fig. 2) penetrated through a section of Darai into Ieru shale, then into a second section of Darai. There was no Toro sandstone encountered in the core of the structure.

The Darai limestone is highly resistive, whereas the Ieru shales and Toro sandstones are far

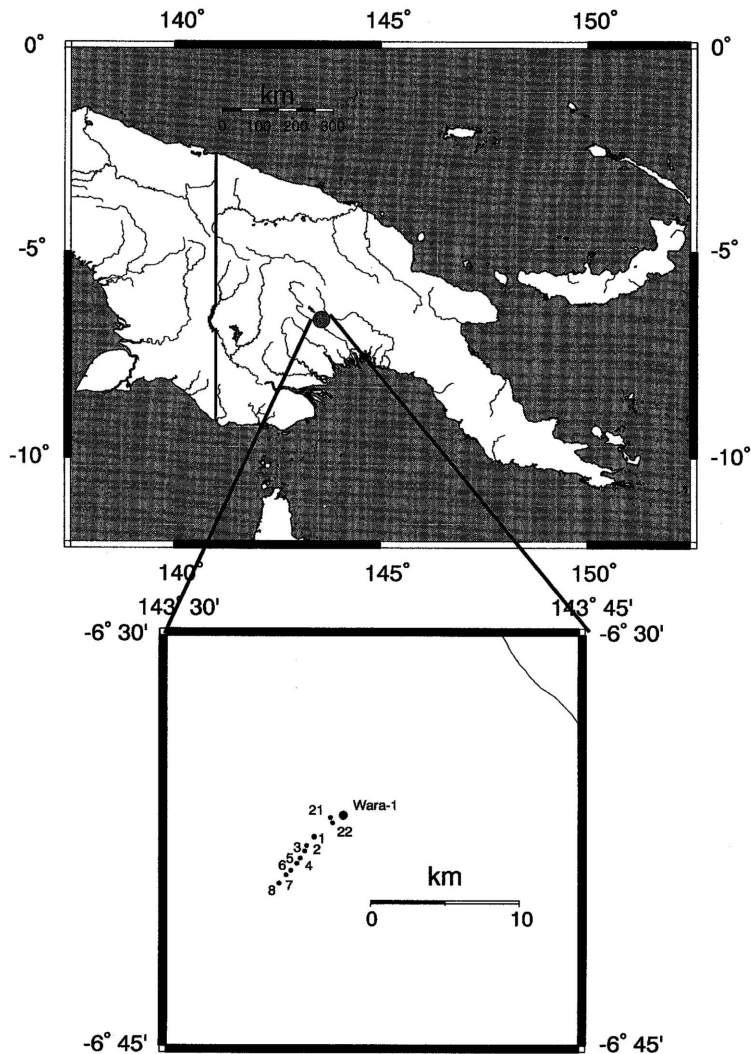


Fig. 2. Location map of the PNG dataset sites. The ten full 5-component MT sites shown as numbered dots. Also shown is the location of the Wara-1 well.

more conductive. Accordingly, the problem seems well-posed for MT to address, with a strong difference in conductivity between the controlling features.

4. Overview of the Papers

4.1 COPROD2

The first two papers in this special issue describe an interpretation (Pous *et al.*, 1997a) and a re-evaluation (Agarwal *et al.*, 1997) of the COPROD2 dataset. This dataset comprises the off-diagonal elements from thirty-five sites crossing the North American Central Plains (NACP) conductivity anomaly (see Jones, 1993b, and references therein). Static shifts have already been applied, and the quest is to seek a 2D model that adequately explains the observations.

A variety of models were shown in Jones (1993b), and all fit the data to varying degrees.

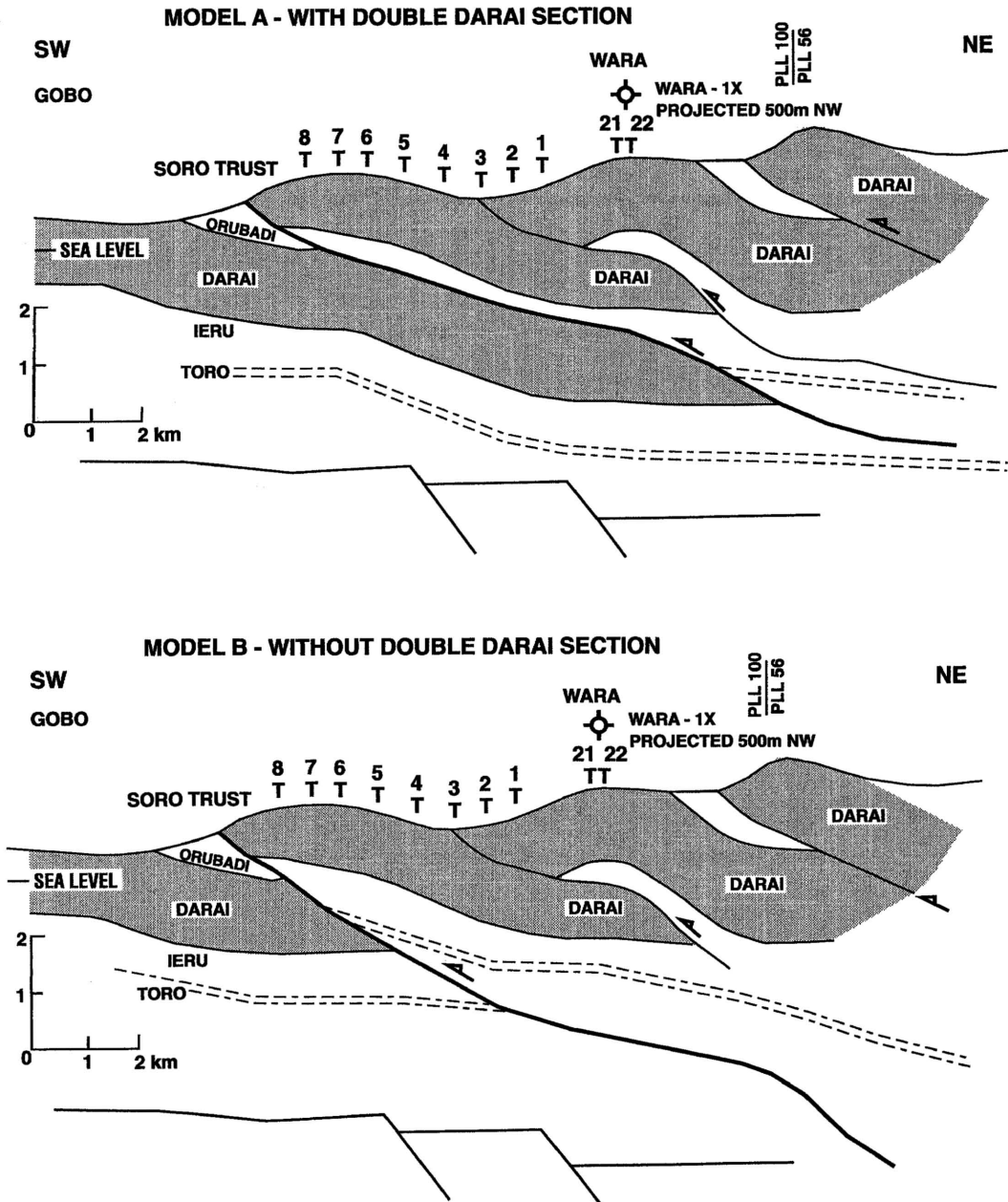


Fig. 3. Two possible models of the structural geometry beneath the PNG dataset sites with the three main geological units, the Darai limestone, the Ieru shale, and the target Toro sandstone, a potential hydrocarbon reservoir. Model A represents thin-skinned thrusting along the Soro Thrust resulting in a double thickness of Darai limestone, and a deeper stratigraphic position for the Toro sandstone. Model B represents thick-skinned thrusting along the Soro Thrust resulting in a single Darai limestone sequence and a shallower depth to the Toro sandstone.

All inversions agreed that there must exist a region of anomalously high conductivity within the middle and lower crust beneath the region. In the main, most inversions resulted in multiple, unconnected conducting bodies, but some gave a large single body as a simplest solution. Jones (1993b) argued subtle features in the data required the former, citing in particular that the one-to-two degree decrease in the TM phase at sites over the anomalies could only be explained by discrete, disconnected bodies.

The model presented in Pous *et al.* (1997a), obtained using forward trial-and-error model fitting, falls into the category of the multiple-body, with four bodies, each of around $1 \Omega\cdot\text{m}$, in the crust. This is somewhat surprising, given that the stated RMS misfit is 3.8° in phase, which is larger than the feature in the data that requires the interpreter or inverse code to separate the conductors. A new result obtained by Pous *et al.* (1997a) is the apparent existence of a conducting body in the lowermost crust and uppermost mantle beneath the centre of the profile.

Agarwal *et al.* (1997) consider carefully the arguments put forward for the requirements for a single body, and conclude that the fine structure of the TM phase can be explained by very minor variations in the sedimentary section above the anomaly. Thus, they suggest that the case for multiple bodies is still in doubt. Clearly, although the COPROD2 data are considered by the induction community to be too easy in terms of exercising the various inversion codes, we can still learn much about the physics of induction from analysing them.

Perplexingly, those codes that purportedly search for minimum structure models, i.e. *Occam* (deGroot-Hedlin and Constable, 1993; Rasmussen, 1993), and its ABIC (Akaike's Bayesian Inference Criterion)-based variant (Uchida, 1993), *AIM* (Ellis *et al.*, 1993), and *RRI* (Wu *et al.*, 1993), all give models that display multiple-bodies rather than a single one. Are those modelling codes all exhibiting problems with the mathematical formulation, such as some form of Gibb's phenomenon? Or is the construct of Agarwal *et al.* (1997) missing some vital information which is implicitly incorporated when the problem is overparameterized? The gauntlet has been thrown down by Agarwal *et al.* (1997)—does anybody wish to pick it up?

4.2 BC87

The following two papers describe analyses of the BC87 dataset (Jones, 1993c). This dataset is quite complicated, and may be beyond the capabilities of present-day methods to interpret fully. Clearly, there are 3D effects at all scales, from electrode effects to distortion by a large resistive batholith, to possible vertical and horizontal offsets in a lower crustal conducting layer (see Jones, 1993c). Ritter and Ritter (1997) examine the vertical field transfer function data, which were hitherto little regarded. The authors show how Hypothetical Event Analysis can be used to extract regional strike directions from the vertical field transfer functions which are affected by local distortions. They demonstrate that the vertical field transfer function data give a strike angle consistent with the MT data of -30° (or 60°). Thin sheet modelling showed that the sites are greatly affected by the presence of the resistive Nelson batholith. Chave and Jones (1997) reprocess the 24 Hz sampling data from the original time series, and determine jackknife errors on the estimates. They show that, in the main, the estimates derived from Phoenix's processing and those from the robust processing compare quite well in the mid-band (5–500 s). At longer periods, the robust results are smoother and have greater frequency-to-frequency consistency. This is due to better control of leverage and outlier effects by the robust controlled-leverage algorithm. However, there is a substantial discrepancy between the error estimates derived parametrically by Phoenix's code compared to the nonparametric jackknife results. The Phoenix estimates are *too small* at periods shorter than about 5 s, i.e., when the number of available estimates is large, and are *too large* at longer periods. Chave and Jones (1997) then attempted combined galvanic and magnetic distortion removal, and determined that the distortion model is statistically inadequate at some frequencies for quite a few sites.

4.3 OKEMAP

The following two papers describe inversions of the OKEMAP dataset using regularized approaches. Uchida (1997a) uses the ABIC statistical criterion to define optimal model smoothness, and inverted the data using three choices for frequency subset and smoothness constraint. All three models have common features which can be considered reliable. They all display a very conductive host formation ($10 \Omega\cdot\text{m}$) in which is embedded two large resistive bodies, of $\sim 100 \Omega\cdot\text{m}$. The paper on the OKEMAP data by Ogawa (1997a) uses the same philosophy as Uchida, but adds static shifts as free parameters. Generally, the static shifts derived are close to unity, but some regions exhibit significant shifts up to a third of an order of magnitude. The final model obtained has less resolution than does Uchida's models, as Ogawa has far fewer model parameters. Gross similarities can be seen between Uchida's and Ogawa's models, but Ogawa's is much smoother in the two regions of large static shifts than are Uchida's. Clearly the message to be learned here is that static shifts must be incorporated into the inversion algorithm.

4.4 PNG

The final six papers all concentrate on the PNG dataset. Lilley (1997) uses Mohr circle analysis to investigate the galvanic distortions of the data, and concludes that five of the ten sites can be characterized as 1D. Four of the remainder show 2D responses, with strike directions close to 120° east of north (-60° west of north). Pous *et al.* (1997b) applied Groom-Bailey distortion analysis to the data, and determined that 120° (-60°) strike was appropriate. Two-dimensional forward modelling of the data rotated into that coordinate system yielded a model with alternating resistive Darai limestones and conductive Ieru and Toro stratigraphic units. The TE mode data between 1 s and 10 s were determined to be most sensitive to the presence of the lower Darai limestone, and sensitivity modelling exercises demonstrated that the lower Darai must exist to fit adequately the observations.

Agarwal and Weaver (1997) use their least-block inversion on the PNG data, after rotating the data into a strike of 120° (or N60W as they refer to it), determined using Swift's procedure. Also, prior to inversion, static shifts were corrected for using the two-step procedure of Berdichevsky *et al.* (1989), used recently by Marquis *et al.* (1995), of (i) matching the long period TE mode apparent resistivity curves for each site so that they match a long period asymptote (in this case to $30 \Omega\cdot\text{m}$ at 682.7 s), and (ii) shifting the TM mode apparent resistivity curves for each site to match their corresponding TE mode curves at the highest frequencies.

The authors acknowledge that they are unable to fit all four responses (apparent resistivities and phases for the two modes) adequately, although they note that their misfit of $\text{RMS} = 6.6$ is real in the sense that an arbitrary error floor was not introduced. They present two best fitting models, one with and one without static shift correction. Significantly, the model from uncorrected data does not display a resistive body that could be considered the lower Darai unit, whereas the model from corrected data exhibits a resistive region beneath the northeastern part of the profile. Sensitivity analyses demonstrate that this body is required by the data corrected for static shifts, and the authors' conclude that the second Darai unit must exist.

Toh and Uyeshima (1997) undertake an exhaustive decomposition analysis of the dataset, and demonstrate well the problems that can arise by using traditional estimators of strike. A strike of -60° was concluded by their analyses. From the decomposed regional impedances, they used a 1D Monte-Carlo scheme to find the models that fit the arithmetic (Berdichevsky) averages, and constructed a 2D model by stitching the 1D models together. This 2D model is shown to fit most of the responses, except those of the TM mode phase in the 10 Hz to 10 s band. They conclude that their 1D modelling exercise suggests that only a "single" Darai layer exists.

Ogawa (1997b) also undertook decomposition analysis, and determined a strike slightly different from all the other analyses, in this case -66° . His conclusion resulted from multi-site and multi-frequency decompositions of the data (McNeice and Jones, 1996). As with his OKEMAP

inversions, Ogawa (1997b) solved simultaneously for the model and static shifts that best-fit the data and was also optimally smooth, determined using ABIC. The inversion was of ten frequencies covering the whole data range, with an error floor for apparent resistivity set to 10%, and an equivalent value for phase, and the model was permitted to have a separate roughness for shallow (<0.5 km) and deep (>0.5 km) structure. The final model showed a single continuous dipping resistive layer interpreted as the Darai limestone. Beneath the southernmost stations (106 and 107) there is a second, deeper resistive layer which may be another thrust sheet of the Darai limestone, but this deeper layer does not underlie the whole profile.

Finally, Uchida (1997b) also undertook ABIC-based 2D smooth inversion of decomposed data at -66° provided by Ogawa (1997b). In contrast to the other models, Uchida (1997b) incorporated the rather severe topography taken from a survey map of the region. Uchida (1997b) inverted the TE+TM, original TM-only, distortion decomposed TM-only, and determinant responses, with an assumed error floor of 3%, and demonstrated that the models resulting from these four are essentially the same. A surface highly resistive layer was interpreted as a 1-km-thick section Darai limestone, underlain by a thick sequence of low-resistivity sedimentary rocks which form the target oil reservoir. A second Darai was not found.

Clearly, for weakly distorted data such as the PNG dataset, many schemes will determine the approximate strike angle, and data rotated into that coordinate system are little different from those derived by distortion decomposition (see, e.g., Uchida, 1997b). It is perhaps surprising that the PNG data are so weakly distorted, given the severe topography of the region. However, careful analysis by Ogawa (1997b) suggested a strike angle that is slightly different from that derived by the other authors, -66° compared to -60° . Does this 6° make a difference? It will not for the larger off-diagonal element (ρ_{\max} and ϕ_{\max}), as sensitivity to strike angle for this element is weak. If the other off-diagonal element is much smaller, however, then (ρ_{\min} and ϕ_{\min}) may be dramatically affected by even a few degrees of rotation. This does not seem to be the case for these data, as they are well-behaved and show smooth “peanut-diagrams” with none of the cusps that indicate severe sensitivity to choice of strike angle. Thus, the models can all be directly compared against each other, even though the strike angles differ a little and some were obtained from rotated data whereas others were obtained from distortion decomposed data.

5. Conclusions

This second MT data interpretation workshop was fruitful in highlighting areas that are now reasonably well established, and areas that still need some work.

For even what appears to be the very simplest of datasets, COPROD2, there are some fundamental questions still being asked. The bulk response is easy to explain, but the subtle features are far more difficult to resolve. BC87 still is beyond the challenge of currently-available methods for interpreting MT data. Clearly there are 3D effects at all scales. OKEMAP data demonstrate the advantage of high spatial sampling. Nevertheless, the statics problem must be addressed properly, rather than by spatial filtering which removes structure.

Finally, a simple question was asked of the PNG dataset—“*Does a second Darai limestone layer exist beneath the survey?*”. The answer derived from the various analyses is equivocal. Pous *et al.* (1997) suggest that it underlies the whole profile, consistent with model A (Fig. 3). Agarwal and Weaver (1997) conclude that it exists only under the northernmost four sites (2, 1, 21, and 22), similar to model B (Fig. 3). Toh and Uchida (1997) resolve only a single Darai layer, which we know from the Wara well is incorrect for at least sites 21 and 22. Ogawa’s (1997b) model is very much like model B, suggesting that the second Darai underlies the southernmost three sites (8, 7 and 6), whereas Uchida (1997b) does not resolve any aspect of a second Darai beneath any part of the line. Of these models, we must note that the one of Pous *et al.* (1997) was obtained by careful trial-and-error forward modelling, taking sensitivity to the existence of the second Darai

layer into account carefully.

Whereas inversion schemes have the attraction of employing objective misfit and regularization criteria, there is a danger of not fitting subtle, significant features when a global misfit is sought. In comparison, detailed forward modelling exercises can be accomplished with due care being given to parts of the responses that are sensitive to the features of interest. This may be the case with the PNG dataset, that the TE responses in the 1–10 s band need to be very carefully fit.

There was an MT-DIW3 at the 1996 Onuma EM induction workshop where a 2D dataset (Kayabe) was analysed. Papers from this workshop will appear in due course in a special issue of *J. Geomag. Geoelectr.* jointly devoted to the Onuma workshop and the MT-DIW3.

There will be an MT-DIW4 prior to the next EM workshop to be held in Romania in 1998. Details can be obtained from Alan Jones (jones@cg.nrcan.gc.ca).

These datasets are readily available for anyone in the induction community to access and to work with. All four are available from the MTNet World Wide Web site on:
<http://www.cg.nrcan.gc.ca/mtnet/data/data.html>
in various formats, including the SEG/EDI format, in impedance format (J-format), and as Geotools database archives.

All contributors to the MT-DIW2 are thanked for their efforts, both at the workshop and also for their patience in waiting for this special issue of *J. Geomag. Geoelectr.* to be published. Yasuo Ogawa greatly aided publishing this special issue. Exxon and Chevron, in particular Charlie Swift (Chevron, U.S.), Bill Robinson (Chevron, Australia) and Len Srnka (Exxon), are thanked for making their industry MT data available to the academic community in order for us to work on “real” problems. Karen Christopherson brought the existence of the OKEMAP dataset to our attention as a possible problem set for the MT-DIW to address. David Wight is thanked for making Geotools available for the duration of the workshop, and for being on-hand to give assistance when required. The convenors thank Margaret Johnston and the staff of the Earth Sciences Department and the Institute of Theoretical Geophysics, University of Cambridge, for their assistance rendered in staging this workshop.

Appendix. Operations Report: Kube Kabe Magnetotelluric Survey, Kube91—Papua New Guinea

The Kube Kabe project was a magnetotelluric (MT) survey undertaken by Zephyr Geophysical Services, Inc. for Chevron Niugini Pty. Ltd. in PPL 100, Southern Highlands, Papua New Guinea. The survey commenced on 12 July 1991 and was completed on 4 August 1991.

The principal objective of the survey was a more complete mapping of thickness of the Darai Limestone in the general vicinity of the Chevron Wara #1 well along the Wara and Kube Kabe Ranges. Data was taken in a full suite of frequencies from 384 Hz down to .001 to .002 Hz. The most important range was primarily from 3 Hz to .05 Hz and using Cascade Decimation in the low frequencies it was possible to concentrate large numbers of samples in this range.

The camp was located near the center of the Gobe Gap, just below an abandoned rig site. The camp itself was a relatively primitive fly camp consisting of two large covered, three sided shelters. The camp was built expressly for the MT survey and furnished by Exploration PNG, Pty. Ltd. It was centrally located for access to the survey area, and approximately five minutes flight time from Kantobo airstrip, and ten minutes flight time from Pimaga airstrip. All of the equipment was flown from Port Moresby via Milne Bay charter flights to Kantobo, Pimaga, or Mendi airstrips, depending on the weather. The equipment was then slung via helicopter from the airstrip to the Gobe camp for operations. Fuel and supplies were flown from Mendi to Kantobo or Pimaga via fixed wing and then slung to camp. One Hughes 500D from Pacific Helicopters was used throughout the survey.

A total of twenty stations were recorded, with stations located along three distinct profiles trending roughly N30E, perpendicular to prevailing structures. The lines were identified as Wara (W) on the west, Masaka (M) in the center, and Wasuma (S) on the east. One central helipad was cut at each picked location, and all equipment and personnel were flown to this spot. The instrument tent was set up near the central helipad, and the sites themselves were installed 200–600 meters on each side of the helipad and recorded as remote referenced pairs. In addition, a set of remote magnetic coils were installed at the Wara rigsite and beamed via telemetry as a third set of reference coils to aid in reducing local noise on the magnetics. Logistics prevented the telemetry from working at several locations, and where the telemetered coils were used, the results did not indicate great improvement. Time series data were recorded at every station. The beginning of the survey was marked by bad flying weather. The crew and a small amount of equipment were in camp and ready to begin operations on 12 July, but bad flying conditions for fixed wing aircraft at Kantobo and Pimaga as well as Chevron cargo priorities caused a delay in arrival of sufficient gear to begin the survey until 19 July. At this time the survey commenced with the Wara line.

Wara (7/19–7/23)

The Wara line started approximately two kilometers SE of the Wara #1 rigsite and was composed of eight stations spaced in pairs along a line approximately S30W. The weather on this line was generally good, with light rain showers daily, but good visibility and no lightning. Stations W01–W04 were in reasonably gentle topography, and stations W05–W08 were in severe Karst sinkhole terrain, with very rugged local topography between stations. Signal levels were generally up while recording this line, and combined with careful site layout and long telluric lines (200 m) data quality overall was excellent. This line shows some of the cleanest MT data ever collected in PNG. The four setups on the Wara line were recorded in four nights and the crew moved to the Wasuma line next.

The stations at the Wara rig site were 400 m west and south of the drillhole, in an attempt to get away from any effect the casing or vertical hole might have on data. The data was marginal after one night of recording, and a second day was spent there. Data quality by the second night was quite good, and after checking at Wasuma again for visibility at S13–S14, equipment was slung to camp and packing begun.

There were a total of 237.5 hours of recording on the survey, with fifteen days of production and two weather days during actual data collection. Helicopter time averaged approximately four hours per day for the MT survey itself plus camp resupply, fuel slinging, moving cutting crew, site scouting, etc. A total of six laborers on the layout crew and 8–10 local laborers on the pad-cutting crew were utilized, with Exploration PNG providing two foremen previously experienced in Zephyr MT operations. At the conclusion of the survey, all equipment was slung to Kantobo and removed via fixed wing to Moro, where it was transferred to Port Moresby for storage.

Station descriptions: Kube Kabe MT survey—July, 1991

All stations were recorded with saltwater/bentonite mixture to help alleviate contact problems associated with limestone outcrop and shallow jungle soil. All stations were in thick double and triple canopy jungle, requiring cut helipads for instruments and drop zones cut at some site locations. Many stations required the use of a 100 ft. long line for slung loads due to the height of the trees.

Wara line

W01/W02

Centrally located helipad approx. 2 km southwest of Wara rigsite. W01 300 m along line N. of helipad, in moderately steep terrain. N. pot downhill at 10 deg. and crosses gully 30 m from

pot. W. pot uphill at 20 deg.—site W02 250 m S. of helipad along line, moderate terrain, S. pot only 20 m length due to steep cliff. N. pot 200 m to compensate length.

W03/W04

W03 approx. 200 m SW. of river, 200 m N. of helipad. Site on relatively flat ground, no unusual topo changes. Site W04 located 300 m SW. of helipad on mild N. facing slope. Telluric lines even in all directions. Good top layer of soil for pots.

W05/W06

W05 along transect 250 m N. of helipad, moderately steep sinkhole terrain. N. pot travels uphill from depression, S. pot uphill also, E. pot across slope and even, W. pot slight uphill. Heavy limestone outcrop. W06 installed on steep sidehill 200 m SW. of helipad, sinkholes 100 m across and 100 m deep all along hillside. Tellurics relatively even overall across averaged ground.

W07/W08

W07 200 m N. of helipad along transect. Steep sinkhole terrain, large (100 m by 200 m) sinkholes with steep sides. Much limestone outcrop. Tellurics run diagonally across slopes as much as possible to minimize effect of topography. W08 in similar terrain, 300 m SW of helipad.

Wara rigsite—W21/W22

W21 400 m W. of rigsite casing, on levelled auxiliary pad. Tellurics run into surrounding slopes, relatively mild slope correction overall. W22 400 m S. of rigsite, on cleared auxiliary pad with no connection to rigsite pad. Tellurics run into surrounding hillside. S. pot down steep (25 deg.) slope, W. pot down steep slope also. N. and E. pots across slope.

REFERENCES

- Agarwal, A. K. and J. T. Weaver, Two-dimensional inversion of Papua New Guinea data using 'least-blocked' models, *J. Geomag. Geoelectr.*, **49**, this issue, 827–842, 1997.
- Agarwal, A. K., K. J. MacDonald, and J. T. Weaver, COPROD2 revisited: can the B-polarization phase distinguish between single- and multi-body anomalies?, *J. Geomag. Geoelectr.*, **49**, this issue, 745–756, 1997.
- Berdichevsky, M. N., L. L. Vanyan, and V. I. Dmitriev, Methods used in the U.S.S.R. to reduce near-surface inhomogeneity effects on deep magnetotelluric sounding, *Phys. Earth Planet. Inter.*, **53**, 194–206, 1989.
- Chave, A. D. and A. G. Jones, Electric and magnetic field galvanic distortion decomposition of BC87 data, *J. Geomag. Geoelectr.*, **49**, this issue, 767–789, 1997.
- deGroot-Hedlin, C. and S. Constable, Occam's inversion and the North American Central Plains electrical anomaly, *J. Geomag. Geoelectr.*, **45**, 985–999, 1993.
- Ellis, R. G., C. G. Farquharson, and D. W. Oldenburg, Approximate inverse mapping inversion of the COPROD2 data, *J. Geomag. Geoelectr.*, **45**, 1001–1012, 1993.
- Hart, D. L., Reconnaissance of the water resources of the Ardmore and Sherman Quadrangles, Southern Oklahoma, *Oklahoma Geol. Survey, Map HA-3, Scale 1:250000*, 1974.
- Jones, A. G., Introduction to MT-DIW1 special section, *J. Geomag. Geoelectr.*, **45**, 931–932, 1993a.
- Jones, A. G., The COPROD2 dataset: Tectonic setting, recorded MT data and comparison of models, *J. Geomag. Geoelectr.*, **45**, 933–955, 1993b.
- Jones, A. G., The BC87 dataset: tectonic setting, previous EM results, and recorded MT data, *J. Geomag. Geoelectr.*, **45**, 1089–1105, 1993c.
- Lilley, F. E. M., A critique of the MTDIW2-PNG data set based on Mohr circles, *J. Geomag. Geoelectr.*, **49**, this issue, 807–815, 1997.
- Marquis, G., A. G. Jones, and R. D. Hyndman, Coincident conductive and reflective lower crust across a thermal boundary in southern British Columbia, Canada, *Geophys. J. Int.*, **120**, 111–131, 1995.
- McNeice, G. and A. G. Jones, Multisite, multifrequency tensordecomposition of magnetotelluric data, Contributed paper at 66th Annual Society of Exploration Geophysics meeting, held in Denver, Colorado, on 10–15 November, Abstract publ. in Expanded Abstracts, **66**, 281–284, 1996.
- Ogawa, Y., Data-adaptive inversion of the Oklahoma EMAP dataset, *J. Geomag. Geoelectr.*, **49**, this issue, 801–806, 1997a.
- Ogawa, Y., Two-dimensional inversion of Papua New Guinea magnetotelluric dataset assuming static shift as a Gaussian distribution, *J. Geomag. Geoelectr.*, **49**, this issue, 857–867, 1997b.
- Pous, J., J. Ledo, A. Marcuello, and P. Queralt, Two-dimensional forward modeling of the NACP anomaly (COPROD2R data), *J. Geomag. Geoelectr.*, **49**, this issue, 739–744, 1997a.
- Pous, J., J. Ledo, A. Marcuello, and P. Queralt, On the resolution of the Darai limestones by two-dimensional MT forward modeling, *J. Geomag. Geoelectr.*, **49**, this issue, 817–825, 1997b.

- Rasmussen, T., Two-dimensional Occam model of COPROD2 data—first order description of resolution and variance, *J. Geomag. Geoelectr.*, **45**, 1027–1037, 1993.
- Ritter, P. and O. Ritter, The BC87 dataset: application of Hypothetical Event Analysis on distorted GDS response functions and some thin sheet modelling studies of the deep crustal conductor, *J. Geomag. Geoelectr.*, **49**, this issue, 757–766, 1997.
- Toh, H. and M. Uyeshima, Two-dimensional model study of the PNG dataset using site-independent Groom-Bailey decomposition, *J. Geomag. Geoelectr.*, **49**, this issue, 843–856, 1997.
- Uchida, T., 2-D inversion of COPROD2 magnetotelluric data by use of ABIC minimization method, *J. Geomag. Geoelectr.*, **45**, 1063–1071, 1993.
- Uchida, T., Two-dimensional inversion of Oklahoma EMAP data with smoothness regularization, *J. Geomag. Geoelectr.*, **49**, this issue, 791–800, 1997a.
- Uchida, T., Two-dimensional inversion of Papua New Guinea magnetotelluric data with smoothness regularization, *J. Geomag. Geoelectr.*, **49**, this issue, 869–878, 1997b.
- Wu, N., J. R. Booker, and J. T. Smith, Rapid two-dimensional inversion of COPROD2 data, *J. Geomag. Geoelectr.*, **45**, 1073–1087, 1993.